J. Chem. Sci. Vol. 123, No. 2, March 2011, pp. 215–228.

Structural models of vanadate-dependent haloperoxidases, their reactivity, immobilization on polymer support and catalytic activities

MANNAR R MAURYA*

Department of Chemistry, Indian Institute of Technology Roorkee, Roorkee 247 667, India
e-mail: rkmanfcy@iitr.ernet.in

Abstract. The design of structural and functional models of enzymes vanadate-dependent haloperoxidases (VHPO) and the isolation and/or generation of species having {$VO(H_2O)$}, {VO_2}, {$VO(OH)$} and {$VO(O_2)$} cores, proposed as intermediate(s) during catalytic action, in solution have been studied. Catalytic potential of these complexes have been tested for oxo-transfer as well as oxidative bromination and sulfide oxidation reactions. Some of the oxidovanadium(IV) and dioxidovanadium(V) complexes have been immobilized on polymer support in order to improve their recycle ability during catalytic activities and turn over number. The formulations of the polymer-anchored complexes are based on the respective neat complexes and conclusions drawn from the various characterization studies. These catalysts have successfully been used for all catalytic reactions mentioned above. These catalysts are stable and recyclable.

Keywords. Vanadium complexes; haloperoxidases; structural models; functional models; catalysts.

1. Introduction

Discovery of vanadium(V) in the active site of vanadate-dependent enzymes, vanadium haloperoxidases[1–3] isolated from various sea algae[4] and terrestrial fungi, has stimulated research on the coordination chemistry of vanadium. These enzymes catalyse the oxidation of halides (X^-), by peroxide as oxidant, to hypohalous acid (HOX) which further halogenates hydrocarbons non-enzymatically according to (1) and (2).

$$X^- + H_2O_2 + H^+ \rightarrow HOX + H_2O, \quad X^- = Cl^-,\ Br^- \text{ and } I^-, \tag{1}$$

$$HOX + RH \rightarrow RX + H_2O, \tag{2}$$

RH = organic substrates, RX = halogenated products.

They also catalyse the oxidation of sulfide to sulfoxide, as

$$RSR' + H_2O_2 \rightarrow RS(O)R' + H_2O. \tag{3}$$

The active centre of vanadate-dependent haloperoxidases (VHPO) is constituted by vanadate(V) covalently linked to the imidazole moiety of a histidine side-chain of the protein where vanadium is in a trigonal-bipyramidal environment, with the imidazole-N and an OH^- in the axial positions.[5–7]

Many vanadium complexes provide a suitable structural and/or functional model for these enzymes.[8–10] Oxidations of aliphatic as well as aromatic substrates[11–14] including organic sulfides to sulfoxides,[15,16] catalysed by vanadium complexes, have also been achieved in excellent yield. Recently, we have directed our investigations into the coordination chemistry of vanadium in its higher oxidation states. Novel structural features and reactivity patterns of these complexes present model character for VHPO. The catalytic potential of oxidovanadium(IV) and dioxidovanadium(V) complexes as mimics for the catalytic activity of VHPO and oxidation of other organic substrates have also been studied.

Generally, these functional models are homogeneous in nature and decompose during the catalytic action and thus are not suitable for potential industrial applications. The stability and recycle ability of these complexes have been improved by immobilizing them onto polymer support. For the development of industrial processes, such modifications to model complexes acting as homogeneous catalysts would be very important and this, in addition, would lead to operational flexibility of the catalyst as well.

*For correspondence

2. Structural models of haloperoxidases

Reaction of $[VO(acac)_2]$ and benzimidazole derived ligands Hsal-ambmz (**I**) or Hsal-aebmz (**II**) (scheme 1) in dry, refluxing methanol gave the brown oxidovanadium(IV) complexes $[V^{IV}O(acac)(sal\text{-}ambmz)]$ (**1**) or $[V^{IV}O(acac)(sal\text{-}aebmz)]$ (**2**), respectively. Aerial oxidation of **1** and **2** in methanol, yielded the dioxidovanadium(V) complexes $[V^{V}O_2(sal\text{-}ambmz)]$ (**3**) and $[V^{V}O_2(sal\text{-}aebmz)]$ (**4**), respectively. Further, **3** and **4** were obtained from the reaction of the respective ligand with aerially oxidized solution of $[VO(acac)_2]$ in methanol. Aerial oxidation of the filtrate obtained after separating **1** resulted in the formation of $[V^{V}O_2(acac\text{-}ambmz)]$ (**5**) and the known complex $[V^{IV}O(sal\text{-}phen)]$ (**6**). Apparently, the formations of these complexes proceed through a complex reaction pattern as depicted in scheme 1.[17] The complex $[V^{V}O_2(acac\text{-}ambmz)]$ (**5**) can also be prepared directly by reacting $[VO(acac)_2]$ with 2-aminomethylbenzimidazole (ambmz) followed by aerial oxidation. Reaction of **4** with H_2O_2 in methanol resulted in the formation of oxidoperoxidovanadium(V) complex $[V^{V}O(O_2)(sal\text{-}aebmz)]$ (**7**).

The existence of two sharp bands in the 888–958 cm^{-1} region in dioxidovanadium(V) complexes suggested a *cis*–VO_2 arrangement.[10] The ^{51}V NMR spectral data of the complexes **3**, **4** and **5** show one strong resonance in the range $\delta = -540$ and -568 ppm due to a mixed O/N donor coordination.[18] These complexes can be considered as structural models of VHPO as they attain a trigonal bipyramid geometry with slight distortion towards the square pyramid, confirmed by single crystal X-ray diffraction studies. The τ-parameters amount to 0.61–0.71, and the bzm-N and O of the acac/sal moiety are in the axis.

A solution of potassium vanadate generated *in situ* by dissolving V_2O_5 in aqueous KOH, reacts with the potassium salts of H_2sal-inh (**III**), H_2sal-nah (**IV**) and H_2sal-fah (**V**) (scheme 2) at pH ca. 7.5 to give the corresponding dioxidovanadium(V)

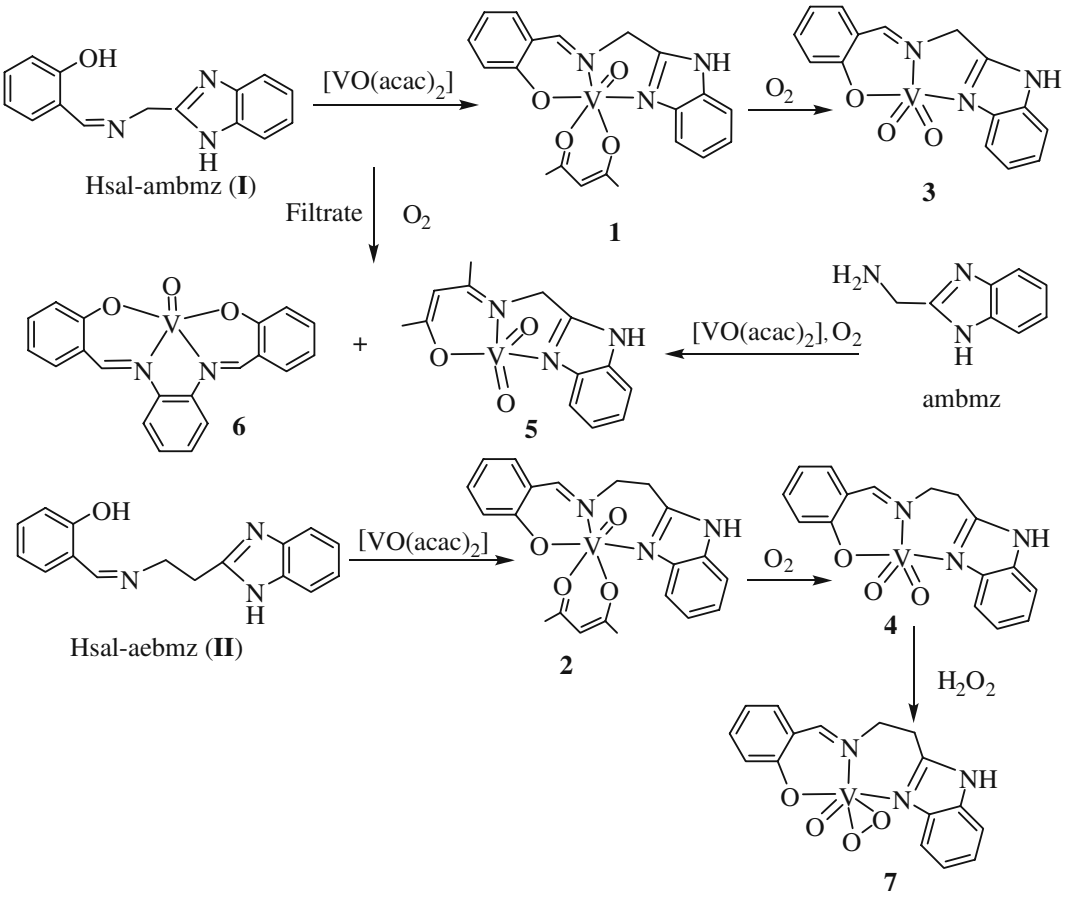

Scheme 1. Synthesis of vanadium complexes.[17]

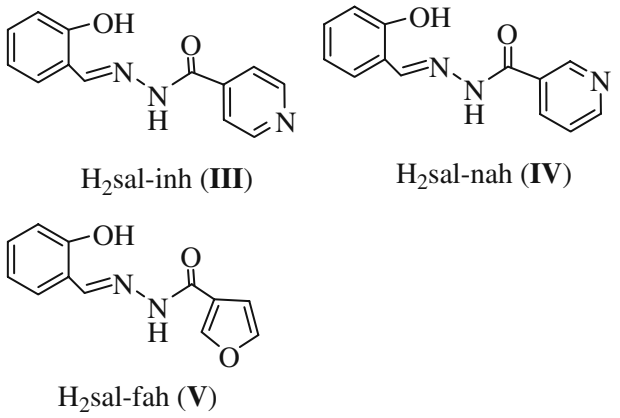

Scheme 2. Ligands used for the synthesis of vanadium complexes.

complexes, $K[V^{V}O_2(sal\text{-}inh)]\cdot H_2O$ (**8**), $K[V^{V}O_2(sal\text{-}nah)]\cdot H_2O$ (**9**), and $K[V^{V}O_2(sal\text{-}fah)]\cdot H_2O$ (**10**).[19,20]

Aqueous solutions of **9**, and **10** further react with $HClO_4$ to yield the neutral complexes $[V^{V}O_2(Hsal\text{-}nah)]$ (**11**) and $[V^{V}O_2(Hsal\text{-}fah)]$(**12**), respectively, in which one of the nitrogens of the =N−N= group is protonated as shown by (4). Such complexes have also been reported by Plass *et al.*[21]

$$K\left[V^{V}O_2L\right]\cdot H_2O + HClO_4 \rightarrow \left[V^{V}O_2\,(HL)\right] + KClO_4 + H_2O \quad (4)$$
$$(H_2L = \textbf{IV} : \textbf{11};\ H_2L = \textbf{V} : \textbf{12}).$$

Slow crystallisation of these protonated complexes from excess methanol causes the removal of the proton from the NH group and conversion to the methoxido-oxidovanadium(V) complexes **13** and **14**, scheme 3.

The formation of complexes **13** and **14** from the corresponding neutral dioxidovanadium(V) complexes in methanol is of interest in the context of vanadium complexes used as oxo-transfer agents both in catalytic and stoichiometric oxygenation reactions.[22]

Conversion of **4** into the peroxido complex **7** by the treatment with H_2O_2 represents the formation of an intermediate similar to that found in the catalytic cycle

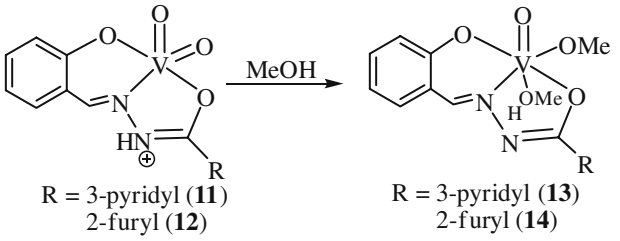

Scheme 3. Reaction of dioxidovanadium(V) complexes with MeOH.[22]

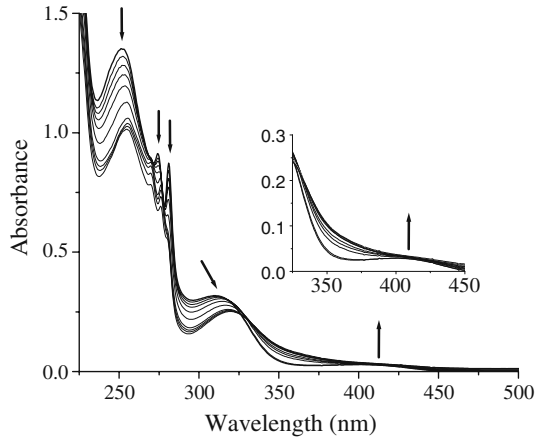

Figure 1. Titration of $[V^{V}O_2(sal\text{-}aebmz)]$ (**4**) with 30% H_2O_2 in MeOH. The spectra were recorded after successive addition of 1-drop portions of H_2O_2 dissolved in MeOH to 10 mL of a ca. 1×10^{-4} M solution of **4**.[17]

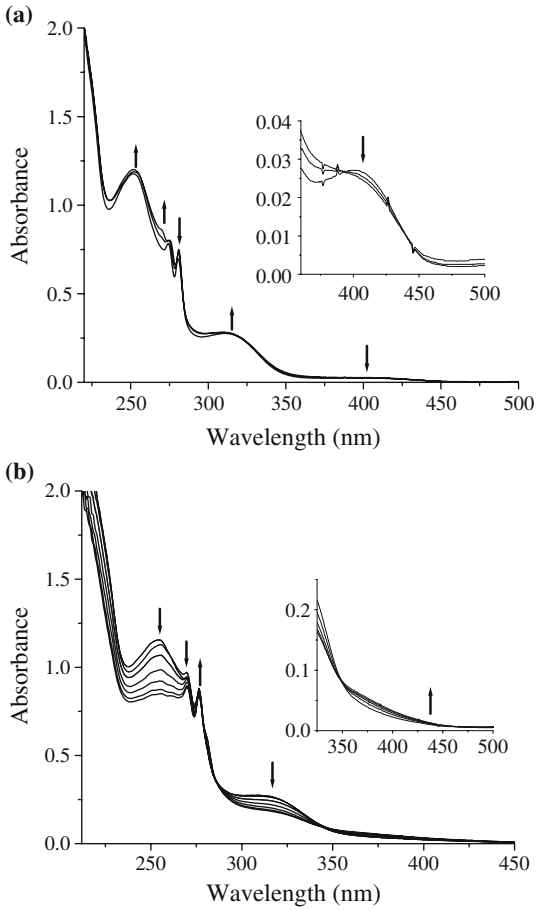

Figure 2. Titration of $[V^{V}O_2(sal\text{-}aebmz)]$ (**4**) with HCl in MeOH. The spectra were recorded after successive addition of 1-drop portions of HCl to 10 mL of ca. 10^{-4} M solution of **4**.[17]

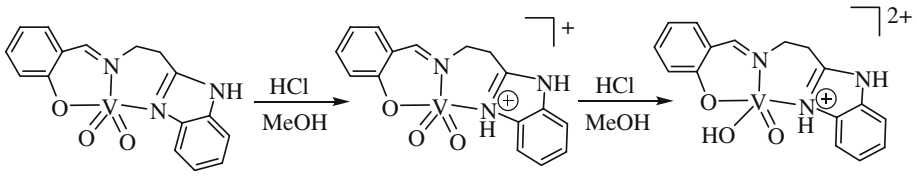

Scheme 4. Reaction of $[V^{V}O_2(\text{sal-aebmz})]$ with HCl dissolved in MeOH.[17]

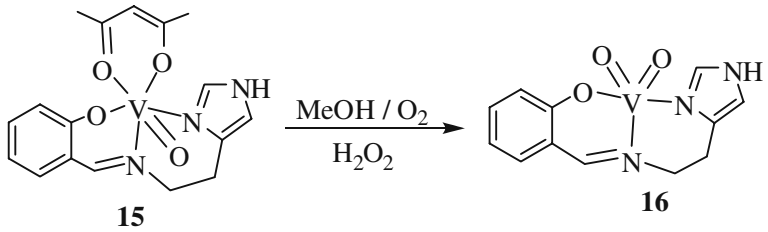

Scheme 5. Oxidation of $[V^{IV}O(\text{acac})(\text{sal-his})]$ by aerial oxygen in MeOH.[28]

of VHPO.[23] The stability of **7** is poor and decomposes slowly at room temperature. However, freshly prepared and dried sample shows three IR active vibrational modes associated with the peroxido moiety $\{V(O_2)^{3+}\}$ at 878, 755 and 614 cm^{-1}, and these are assigned to the O–O intra-stretch (ν_1), the antisymmetric $V(O_2)$ stretch (ν_3), and the symmetric $V(O_2)$ stretch (ν_2), respectively. The presence of these bands confirms the common η^2-coordination of the peroxido group.[24] In addition, the complex exhibits an intense $\nu(V=O)$ stretch at 965 cm^{-1}.[25] The formation of the peroxido complex **7** has also been established in solution by the treatment of **4** with H_2O_2 and following the changes by electronic absorption spectroscopy. Thus, drop-wise addition of aqueous 30% H_2O_2 dissolved in methanol to 10 mL of a ca. 10^{-4} M solution of **4** resulted in spectral changes as presented in figure 1. The band appearing at 405 nm slowly broadens (see inset of figure 1), while the band at 313 nm shifts to 321 nm along with a decrease in intensity. Concomitantly, the bands at 273 and 281 nm split into three bands and appear at 269, 276 and 279 nm along with a marginal decrease in intensity. With considerable loss in intensity, the 212 nm band remains constant, while the 252 nm band shifts marginally to 256 nm. The final spectrum is similar to that recorded for the isolated peroxido complex **7**.

Model studies have also been carried out for protonating and deprotonating the complex $[V^{V}O_2(\text{sal-aebmz})]$ (**4**). At least two sets of spectral patterns were observed on addition of methanolic HCl to a solution of **4** in the electronic absorption spectra; figure 2. In the first set, the band at 405 nm shows a slight broadening with a decrease in intensity (inset in figure 2(a)), while the intensity and band position of 313 nm band remains constant. With an increase in intensity, the band at 252 nm registers no change, the 273 nm band shifts to 276 nm, with increase in intensity, while the 281 nm band exhibits a gradual shift towards 280 nm with decrease in intensity. The second set of spectral pattern starts on addition of more HCl and are presented in figure 2(b). These spectral changes have been interpreted in terms of the formation of an oxidohydroxido complex of composition $[V^{V}O(OH)(\text{sal-aebmz})]^{2+}$ via $[V^{V}O_2(\text{sal-aebmzH})]^{+}$, scheme 4.

The solution acquired the original spectral pattern on addition of a methanolic solution of KOH; the reaction is thus reversible. This reversibility is an important observation in the context of the active site structure and the catalytic activity of vanadate-dependent haloperoxidases, for which a hydroxido-ligand at the vanadium centre has been made plausible on the basis of X-ray diffraction data.[23,26] The generation of similar oxido-hydroxidovanadium complexes on acidification of $K[V^{V}O_2(\text{sal-inh})]\cdot H_2O$ (**8**), $K[V^{V}O_2(\text{sal-nah})]\cdot H_2O$ (**9**) and $K[V^{V}O_2(\text{sal-fah})]\cdot H_2O$ (**10**) has also been demonstrated.

The oxidovanadium(IV) complex $[V^{IV}O(\text{acac})(\text{sal-his})]$ (**15**) (where Hsal-his, **VI** = Schiff base derived from salicylaldehyde and histidine) has been reported by Cornman *et al.*[27] Aerial oxidation of **15** in the presence of a few drops of aqueous 30% H_2O_2 results in the

formation of dioxidovanadium(V) complex [$V^{V}O_2$(sal-his)] (**16**), scheme 5.[28] Solution of **15** in methanol is also sensitive towards the addition of H_2O_2, as monitored by electronic absorption spectroscopy, yielding oxidoperoxido species; figure 3. Thus, the progressive addition of a dilute H_2O_2 solution in methanol to a solution of **15** in methanol results first in flattening of the d–d band appearing at 776 nm and finally disappears. The 532 nm band slowly broadens with increase in intensity and finally disappears. The band at 382 nm gradually shifts to 394. At the same time two new bands appear at 319 and 257 nm, while the intensity of the 265 nm band also increases. The disappearance of d–d bands is in accordance with the oxidation of the $V^{IV}O$-complex to an oxidoperoxidovanadium(V), and the appearance of a weak but new band at ca. 425 nm is probably due to a LMCT band of the monoperoxido complex. The spectral changes during a similar titration of **16** in methanol with H_2O_2 (diluted in methanol) demonstrate the formation of same oxidoperoxidovanadium(V) species.

Similarly, the reaction of [$VO(acac)_2$] with an equimolar amount of Hsal-aepy (Hsal-aepy, **VII** = Schiff base derived from salicylaldehyde and 2-aminoethylpyridine or Hsal-dmen (Hsal-dmen, **VIII** = Schiff base derived from salicylaldehyde and N,N-dimethylethylenediamine) in solvent at room temperature yielded the oxidovanadium(IV) complexes [$V^{IV}O$(acac)(sal-aepy)] (**17**) and [$V^{IV}O$(acac)(sal-dmen)] (**19**), respectively. Complexes [$V^{V}O_2$(sal-aepy)] (**18**) and [$V^{V}O_2$(sal-dmen)] (**20**) were then obtained by aerobic oxidation of **17** and **19**, respectively, in solvent in the presence of a small amount of H_2O_2, scheme 6. Single crystal X-ray diffraction studies confirm the mononuclear distorted octahedral structure for **17**[29] and **19**[30] while distorted square pyramidal for **20**.[30]

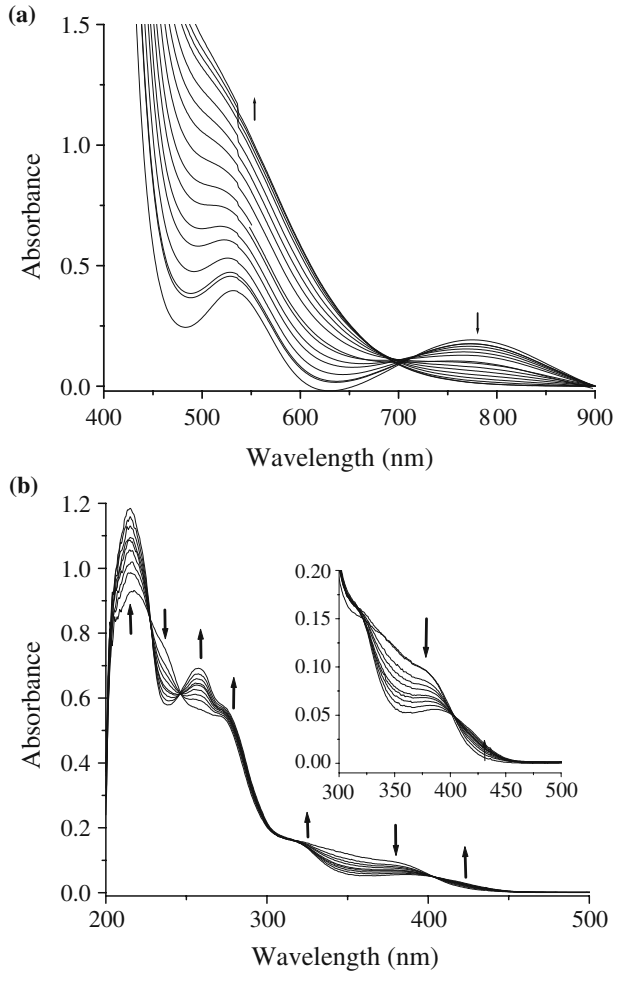

Figure 3. UV-Vis spectral changes observed during titration of [$V^{IV}O$(acac)(sal-his)] (**15**) with H_2O_2. (**a**) The spectra were recorded after successive additions of one drop portions of H_2O_2 (6.6×10^{-4} mmol of 30% H_2O_2 dissolved in 10 mL of methanol) to 50 mL of ca. 10^{-3} M solution of **15** in methanol. (**b**) The equivalent titration, but with lower concentrations of a **15** solution (ca. 10^{-4} M); the inset shows an enlargement of the 300–500 nm region.[28]

3. Immobilization of model vanadium complexes on polymer support

Immobilization of active metal complexes has evolved as a promising strategy for combining the advantages of homogeneous as well as heterogeneous catalysts, due to their easy separation from the products by simple filtration, and to meet the industrial demand of recyclability for continuous operation.[31,32] Catalytic potentials of polymer-immobilized metal complexes in organic transformations have been reviewed in detail by several groups.[33–37]

Various methods have been followed, depending on the nature of ligand, for immobilization of model vanadium complexes on polymer support. Reaction of imidazolomethylpolystyrene (PS-im) with dioxidovanadium(V) complexes K[$V^{V}O_2$(sal-inh)]·H_2O (**8**) and K[$V^{V}O_2$(sal-fah)]·H_2O (**10**) dissolve in DMF gave imidazolomethylpolystyrene bound dioxidovanadium(V) complexes, PS-K[$V^{V}O_2$(sal-inh)(im)] (**21**) and PS-K[$V^{V}O_2$(sal-bhz)(im)] (**22**), respectively, scheme 7.[38] The energy dispersive X-ray (EDX) analyses supported the presence of 1.2% and 1.0% vanadium in **21** and **22**, respectively.

Immobilization of [$V^{IV}O$(acac)(sal-his)] (**15**) to give PS–[$V^{IV}O$(acac)(sal-his)] (**23**) involved the reaction of Hsal-his (**VI**) with chloromethylated polystyrene, cross-linked with 5% divinylbenzene in DMF in the presence of triethylamine followed by reaction of

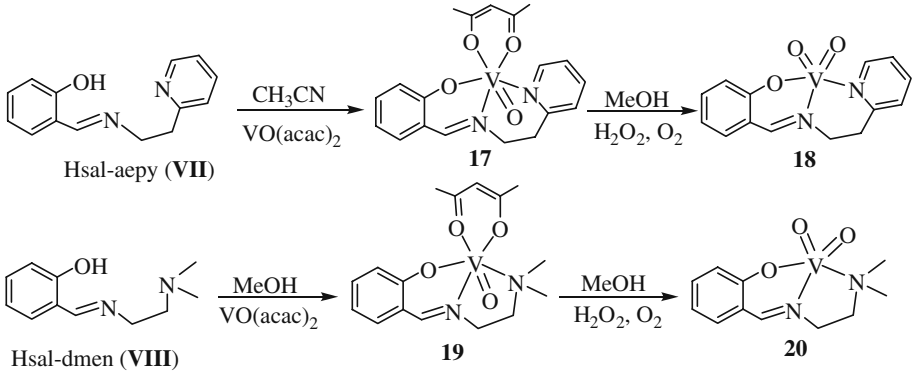

Scheme 6. Scheme for the synthesis of oxidovanadium(IV) and dioxidovanadium(V) complexes.[29,30]

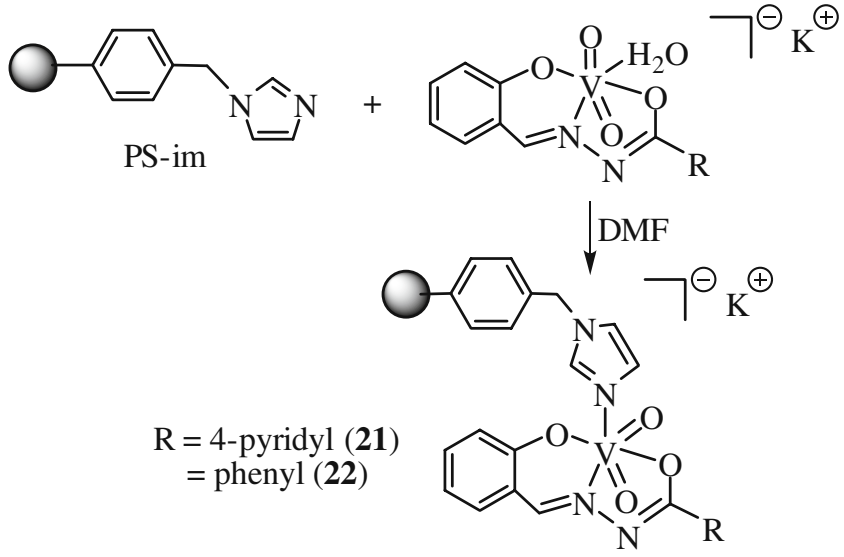

Scheme 7. Ball (●) represents the polystyrene matrix.[38]

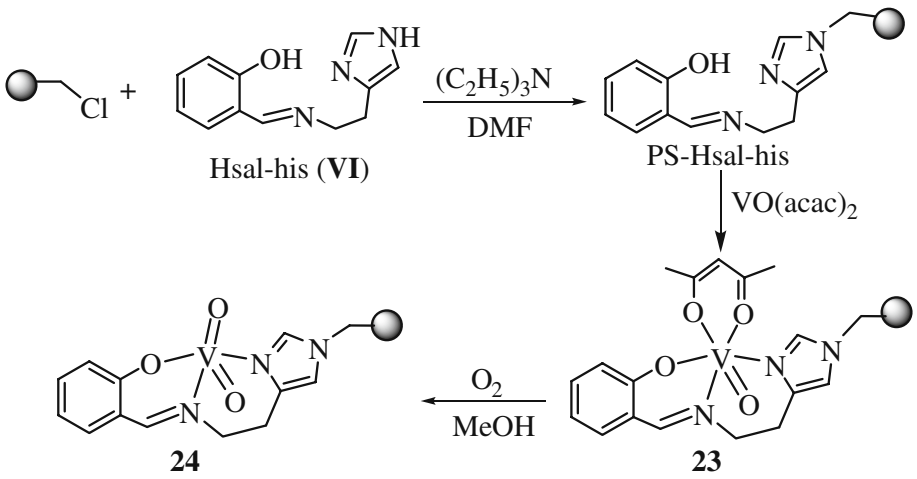

Scheme 8. Scheme for the synthesis of polymer-supported complexes.[28]

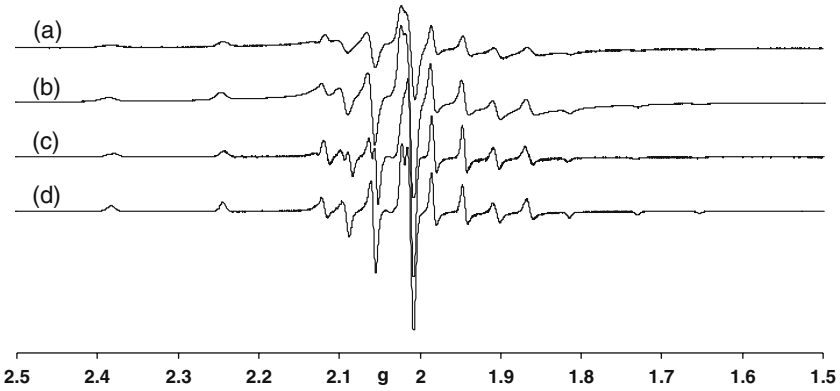

Figure 4. 1st derivative EPR spectra of PS–[V^{IV}O(acac)(sal–his)] (**23**): (a) solid at room Temperature, (b) in contact with DMF at 77 K; and [VO^{IV}(acac)(sal–his)] (**15**): (c) in MeOH at 77 K, (d) in DMF at 77 K.[28]

Table 1. Spin Hamiltonian parameters obtained for [VO^{IV}(acac)(sal–his)] (**15**) and PS-[VO^{IV}(acac)(sal–his)] (**23**).[28]

Complex	Solvent	$g_{\|\|}$	$A_{\|\|}$ ($\times 10^4$ cm^{-1})	$g_\perp$	$A_\perp$ ($\times 10^4$ cm^{-1})
PS–[V^{IV}O(acac)(sal-his)] (**23**)	Solid	1.949	163.8	1.980	58.6
	DMF	1.952	164.8	1.980	57.5
[V^{IV}O(acac)(sal-his)] (**15**)	MeOH	1.953	161.5	1.981	56.0
	DMF	1.954	161.5	1.980	55.7

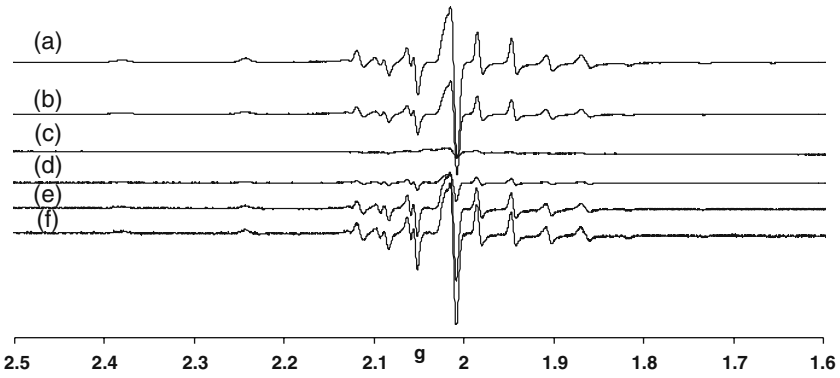

Figure 5. Treatment of compound [VO^{IV}(acac)(sal-his)] (**15**) with 30% H_2O_2 followed by the addition of methyl phenyl sulfide; (a) in MeOH; (b) 0.5 equiv. H_2O_2; (c) 2.0 equiv. H_2O_2; (d) 1.0 equiv. methyl phenyl sulfoxide; (e) 2.0 equiv. methyl phenyl sulfoxide; (f) 2.0 equiv. methyl phenyl sulfoxide (after 20 h) at 77 K.

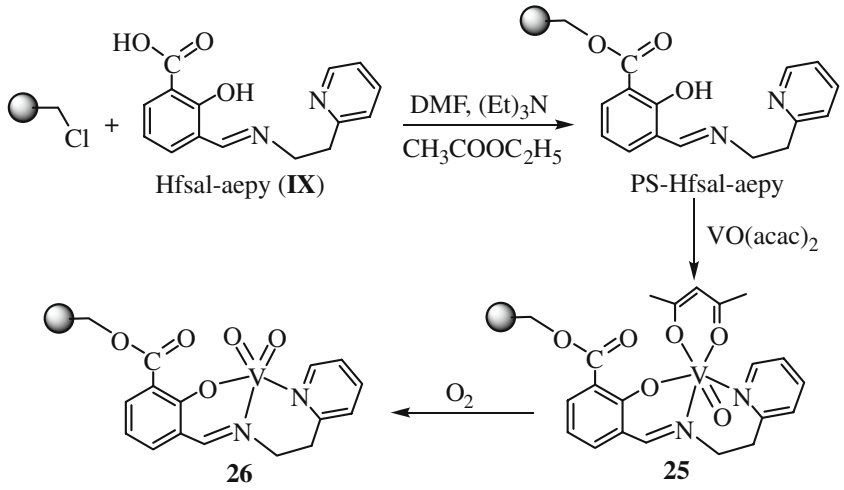

Scheme 9. Scheme for the synthesis of polymer-supported complexes.[29]

Table 2. Spin Hamiltonian parameters obtained for [$V^{IV}O$(acac)(sal-aepy)] (**17**) and PS-[$V^{IV}O$(acac)(sal-aepy)] (**25**).[29]

Complex	Solvent	$g_{\|\|}$	$A_{\|\|}$ ($\times 10^4$ cm^{-1})	$A_{\perp}$ ($\times 10^4$ cm^{-1})	$g_{\perp}$
PS-[$V^{IV}O$(acac)(fsal-aepy)] (**25**)	Solid	1.945	167.6	59.3	1.979
	DMSO	1.946	168.8	58.4	1.980
[$V^{IV}O$(acac)(sal-aepy)] (**17**)	DMSO	1.953	163.5	57.8	1.981
	MeOH	1.952	163.5	A_x 58.6, A_y 57.1	g_x 1.982, g_y 1.981

$VO(acac)_2$ in DMF with the obtained polymer supported ligand. Aerial oxidation of **23** in methanol gave the dioxidovanadium(V) complex PS–[$V^{V}O_2$(sal-his)] (**24**), scheme 8.[28]

The EPR spectra of PS–[$V^{IV}O$(acac)(sal-his)] (**23**) and [$V^{IV}O$(acac)(sal-his)] (**15**) are shown in figure 4. The spectrum of **23** is characteristic of magnetically dilute $V^{IV}O$-complex and the well-resolved EPR hyperfine features indicate that the vanadium(IV) centers are well-dispersed in the polymer matrix. Comparison of the spectra of **23** and **15** indicates that the coordination environment are the same in both complexes and the binding modes of these are also same in DMF solution, as well as in the solid state, table 1 (figure 5).

A very similar procedure, as mentioned above was applied in isolating complex PS-[$V^{IV}O$(acac)(fsal-aepy)] (**25**). Here, carboxylic group on salicylaldehyde of Hfsal-aepy (**IX**) reacted with chloromethylated polystyrene to give polymer-supported ligand as shown in scheme 9. Its dioxidovanadium(V) analogue PS-[$V^{V}O_2$(fsal-aepy)] (**26**) was prepared by aerial oxidation of PS-[$V^{IV}O$(acac)(fsal-aepy)] in MeOH. Hamoltonian parameters obtained for neat as well as polystyrene-supported complexes (table 2) are very similar to those reported above in table 1.[29]

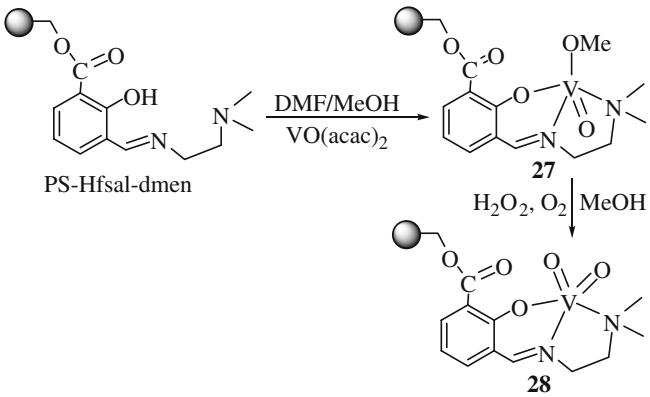

Scheme 10. Formation of PS-[$V^{IV}O$(OMe)(fsal-dmen)] (**27**) and PS-[$V^{V}O_2$(fsal-dmen)] (**28**).[30]

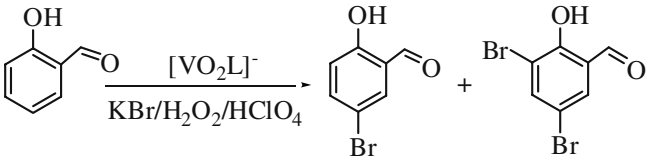

Scheme 11. Oxidative bromination of salicylaldehyde.

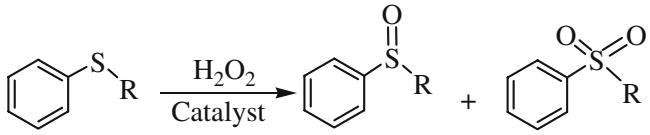

R = CH_3: Methyl phenyl sulfide
R = C_6H_5: Diphenyl sulfide

Scheme 12. Oxidation products of sulfides.[17]

Ligand PS-Hfsal-dmen on reaction with $VO(acac)_2$ gave PS-[$V^{IV}O$(OMe)(fsal-dmen)] (**27**) which on oxidation gave the expected $V^{V}O_2$-complex, PS-[$V^{V}O_2$(fsal-dmen)] (**28**), scheme 10. The presence of MeO^- in PS-[$V^{IV}O$(OMe)(fsal-dmen)] was confirmed by GC-MS on keeping it in DMSO for ca. 15 h and detecting MeOH in liquid part of the mixture.[30]

4. Catalytic activity

4.1 *Oxidative bromination of salicylaldehyde*

The model vanadium complexes have been used as functional models successfully. Thus, K[VO_2(sal-inh)]·H_2O (**8**) and K[VO_2(sal-fah)]·H_2O (**10**) catalyse the oxidative bromination, by H_2O_2, of salicylaldehyde to afford 5-bromo and 3,5-dibromosalicylaldehyde, scheme 11. During this process vanadium reacts with one or two equivalents of H_2O_2, forming monoperoxido {$VO(O_2)^+$} or *bis*(peroxido) {$VO(O_2)^-$} species, which ultimately oxidise bromide, possibly via a hydroperoxido intermediate. The oxidised bromine species (Br_2, Br_3^- and/or HOBr) then brominates the substrate.[4,7,8]

Maximum conversion of salicylaldehyde (ca. 51%) was achieved with 4 mmol of $HClO_4$, 2 mmol of substrate, 15 mmol of H_2O_2, 0.020 g (ca. 0.05 mmol) of catalyst and 0.476 g (4 mmol) of KBr. GC and GC-MS analysis of the crude products obtained under optimised conditions gave 85.8% 5-bromosalicylaldehyde, 9.0% 3,5-dibromosalicylaldehyde and 5.2% of other, unidentified, products. Polymer-supported complexes PS-K[VO_2(sal-inh)(im)] (**21**) and PS-K[VO_2(sal-bhz)(im)] (**22**) gave better conversion.[38] They are more selective also towards the formation of 5-bromosalicylaldehyde, table 3. These catalysts demonstrate their practical applications as they have relatively high turn over frequency and not much loss in the catalytic activities on recycling.

Table 3. Conversion and selectivity data for salicylaldehyde after 2 h of contact time.[38]

Catalyst	% Conv.	TOF (h^{-1})[e]	% Selectivity	
			5-Brsal	Other
8	53.8	60.2	87.3	12.7
10	50.5	61.8	85.3	14.7
21	85.2	775	90.4	9.6
21[a]	81.4	-	90.0	10.0
21[b]	78.6	-	87.0	13
21[c]	77.8	-	86.8	13.2
21[d]	77.1	-	87.0	13.0
22	81.7	800	89.6	10.4
22[a]	78.7	-	87.6	12.4
22[b]	76.1	-	86.4	13.6
22[c]	75.5	-	86.0	14.0
22[d]	75.0	-	86.0	14.0

[a]First cycle of used catalyst
[b]Second cycle of used catalyst
[c]Third cycle of used catalyst
[d]Forth cycle of used catalyst
[e]TOF values in moles of product per mole of catalyst

4.2 *Oxidation of sulfides (thioethers) and other sulphur compounds*

Vanadate-dependent haloperoxidases catalyse the oxidation, by H_2O_2, of sulfides (thioethers) to sulfoxides and further to sulfones.[7,8,39] We have tested the catalytic potential of complexes [V^VO_2(sal-ambmz)] (**3**), [V^VO_2(sal-aebmz)] (**4**), [V^VO_2(acac-aebmz)] (**5**), [V^{IV}O(acac)(sal-his)] (**15**) and [V^VO_2(sal-his)] (**16**) to mimic the sulfide-peroxidase activity of the enzyme.[17,28] Methyl phenyl sulfide and diphenyl sulfide have electron-rich sulfur atoms which on electrophilic oxidation give monosulfoxide, and upon further oxidation disulfoxide, scheme 12. Catalysts PS–[V^{IV}O)(acac)(sal-his] (**23**) and PS–[V^VO_2(sal-his)] (**24**) have also been tested for the oxidation of two sulfides. Table 4 compares the conversion of sulfides, TOF and product selectivity data under optimized conditions. As shown in table, conversions of both sulfides using neat complexes are very good, but always lower than their polymer-bound analogues. The selectivity of the formation of the corresponding monosulfoxide is also lower with neat complexes. Blank reaction taking methyl phenyl sulfide (1.24 g, 10 mmol), aqueous 30% H_2O_2 (1.71 g, 15 mmol) and acetonitrile (15 mL) resulted in 15.2% conversion with sulfoxide: sulfone selectivity of 68 : 32. Blank reaction for diphenyl sulfide under above reaction conditions gave only 5.5% conversion with sulfoxide: sulfone selectivity of 57 : 43.

Step-wise addition of 2 equiv. H_2O_2 (0.5, 1, 1.5 and 2 equiv.) to a methanolic solution of [V^{IV}O(acac)(sal-his)] causes the decrease in the intensity of the EPR spectrum, and after the addition of the 2 equiv. of H_2O_2 the EPR intensity becomes ca. 1/5th of that of the initial solution. The ^{51}V NMR of these solutions confirmed the presence of vanadium(V) species. Subsequent addition of 2 equiv. methyl phenyl sulfide originated spectrum with the same values of g and A parameters, the EPR signal increasing to ~50% of the initial solution, indicating the reversibility of the redox process occurring during the catalytic reaction.

Successive additions of 30% H_2O_2, the relative intensity of the $\delta = -547$ ppm resonance due to [V^VO_2(sal-his)] decreases, and after the addition of 1.5 equiv of H_2O_2, a peak at $\delta = -579$ ppm, appeared due to the formation of [$V^VO(O)_2$(sal-his)] (**29**). However, restoration of original signal upon addition of methyl phenyl sulfide to the above solution confirms the reversibility of the reaction. Original spectrum can also be obtained

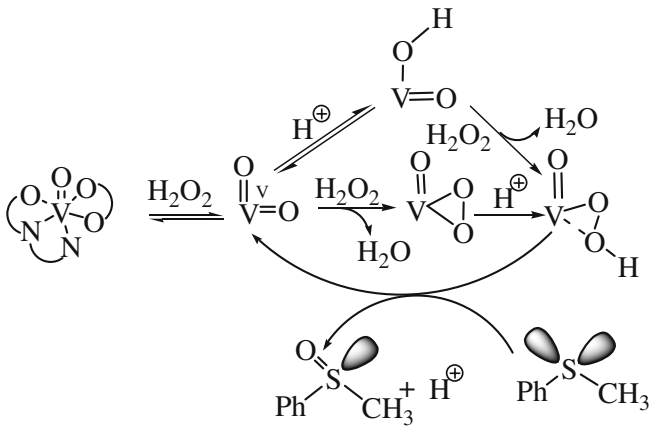

Scheme 13. Reaction mechanism of oxidation of methyl phenyl sulfide as a model substrate for sulfoxidations.

Table 4. Conversion of sulfides, TOF and product selectivity data.[28]

Substrate	Catalyst	Conv. (%)	TOF (h^{-1})	% Selectivity	
				Sulfoxide	Sulfone
Methyl phenyl sulfide[a]	**15**	72.1	83.3	62.9	37.1
	16	84.8	96.4	61.0	39.0
	23	79.5	91.2	64.8	35.2
	24	93.8	113.8	63.7	36.3
Diphenyl sulfide[b]	**15**	60.3	19.8	68.9	31.1
	16	70.7	30.2	67.8	32.2
	23	67.4	28.7	73.1	26.9
	24	83.4	37.5	71.8	28.2

[a]Reaction conditions for polymer-anchored complexes: methyl phenyl sulfide (10 mmol), catalyst (0.025 g), H_2O_2 (1.71 g, 15 mmol) and CH_3CN (15 mL). Neat complexes use same mole concentration as used for the polymer-anchored complexes.
[b]Reaction conditions for polymer-anchored complexes: diphenyl sulfide (10 mmol), catalyst (0.045 g), H_2O_2 (3.42 g, 30 mmol) and acetonitrile (15 mL). Neat complexes use same mole concentration as used for the polymer-anchored complexes.

Table 5. Desulfurization of organosulfur compounds and reaction products.[30]

Catalyst[a]	Sulfur-containing compound	Sulfur content (in ppm)		Sulfur removal (%)
		Initial amount	After desulfurization	
19	Thiophene	500	148.5	70.3
19	Benzothiophene	500	144.5	71.1
19	Dibenzothiophene	500	141.5	71.7
19	2-Methylthiophene	500	140.5	71.9
27	Thiophene	500	65.5	86.9
27	Benzothiophene	500	63	87.4
27	Dibenzothiophene	500	60.5	87.9
27	2-Methylthiophene	500	57.5	88.5
20	Thiophene	500	113	77.4
20	Benzothiophene	500	109.5	78.1
20	Dibenzothiophene	500	111.5	77.7
20	2-Methylthiophene	500	108	78.4
28	Thiophene	500	9.5	98.1
28	Benzothiophene	500	8.5	98.3
28	Dibenzothiophene	500	8	98.4
28	2-Methylthiophene	500	6	98.8

[a]Reaction conditions: Organosulfur compound (500 ppm) in heptane, 30% H_2O_2 (oxidant:substrate molar ratio of 3 : 1) at 60°C.

upon standing the solution having **29** for longer time. The peroxido-complexes being stable and detectable, it is likely that hydroperoxidovanadium(V) complexes also form as aqueous H_2O_2 is being added and the pH decreases, enhancing the electrophilicity of the peroxido intermediate. The peroxide thus activated is subjected to a nucleophilic attack by the sulfide as shown in scheme 13.[40,41]

The removal of sulfur compounds from petroleum products has attracted attention of researchers to fulfill the demand of environment friendly fuels. The oxidation of model organosulfur compounds with sulfur concentrations of 500 ppm was tested in heptane using catalysts PS-[$V^{IV}O$(OMe)(fsal-dmen)] (**27**) and PS-[$V^{V}O_2$(fsal-dmen)] (**28**) in the presence of 30% H_2O_2. The results are summarized in table 5. It is clear from the table that polystyrene-supported catalysts are significantly more effective in oxidizing organic sulfur than their corresponding neat complexes. In addition, the supported catalysts have advantages of being more easily recovered from the reaction mixture.[30]

4.3 *Oxidation of styrene*

Complexes [VO_2(sal-ambmz)] (**3**), [VO_2(sal-aebmz)] (**4**) and [VO_2(acac-aebmz)] (**5**), also catalyse the oxidation of styrene and the major oxidation products obtained are styrene oxide, benzaldehyde, benzoic acid and 1-phenylethane-1,2-diol, scheme 14.[17] Table 6 summarizes the percentage conversion of styrene, the turn over rates, and the selectivities for the various reaction products under optimized reaction conditions.

With H_2O_2, these catalysts are more selective towards benzaldehyde (74–90%), than styrene oxide (5.5–11%), an expected product. The conversion of styrene is though low with TBHP, the selectivity of the formation of styrene oxide is much better than in the case of H_2O_2. Due to the strong oxidizing nature of H_2O_2, the styrene oxide formed in the first step by epoxidation is mainly converted into benzaldehyde via the intermediate hydroperoxistyrene. Benzaldehyde formation may

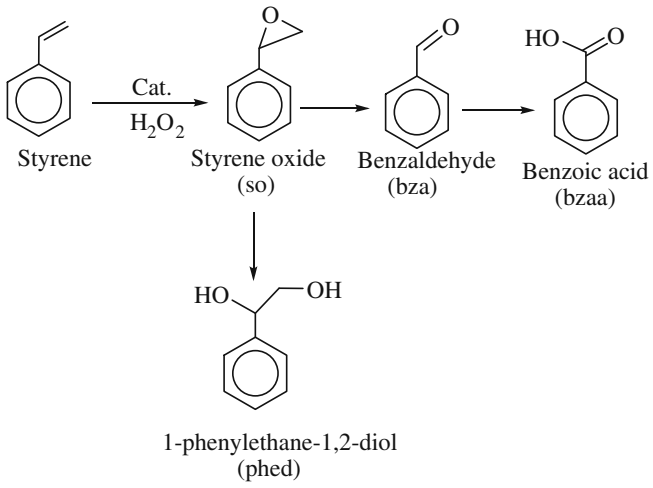

Scheme 14. Various oxidation products of styrene.

Table 6. Percentage conversion of styrene and selectivity for various oxidation products after 6 h of reaction time.[17]

Catalyst	Oxidant	Conv. (%)	TOF (h^{-1})	Product selectivity[a]			
				so	bza	bzaa	phed
3	H_2O_2	51	8.5	5.5	90	0.5	4
4	H_2O_2	55	7.6	11	74	9	6
5	H_2O_2	59	6.6	10	82	5	3
3	TBHP	20	2.6	47	52	1	-
4	TBHP	31	4.3	43	50	5	2
5	TBHP	35	5.1	37	53	8	2

[a]so = styrene oxide, bza = benzaldehyde, bzaa = benzoic acid and phed = 1-phenylethane-1,2-diol.

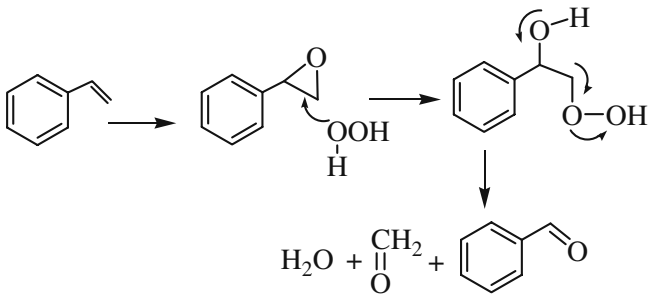

Scheme 15. Proposed mechanism.

also be facilitated by direct oxidative cleavage of the styrene side chain double bond via a radical mechanism, scheme 15.[42] Water present in H_2O_2 is probably responsible for the hydrolysis of styrene oxide to form 1-phenylethane-1,2-diol to some extent. Formation of other products, e.g., benzoic acid through oxidation of benzaldehyde is extremely slow.

4.4 *Hydroamination of styrene and vinyl pyridine*

Transition metal catalysed hydroamination (scheme 16) of olefins has attracted much attention in the past decades due to the ubiquity of the amine functionality in natural products, biological systems, pharmaceuticals and fine chemicals.[43–46]

Hydroamination of styrene and vinyl pyridine catalysed by polymer-anchored complexes, PS-[$V^{IV}O$(acac)(fsal-aepy)] (**25**) and PS-[$V^{V}O_2$(fsal-aepy)] (**26**) gave the corresponding enamines, scheme 17. The Markovnikov and anti-Markovnikov products were separated by column liquid chromatography and confirmed by ^{1}H NMR spectroscopy. Table 7 presents data on hydroamination, turn over frequency (TOF) of the catalyst, and selectivity of the Markovnikov and anti-Markovnikov products obtained under optimsed conditions.[29] The yield of the anti-Markovnikov products are, in general, higher than those of the Markovnikov products. This is possibly due to the steric hindrance imposed by the amine, which decreases the formation of the Markovnikov products.

The catalytic activity of the neat complexes [$V^{IV}O$(acac)(sal-aepy)] (**17**) and [$V^{V}O_2$(sal-aepy)] (**18**) were also tested for the hydroamination of styrene, table 7. It is clear from the table that the neat complexes exhibit slightly lower conversion than the anchored analogue for all reactions. The improvement in the catalytic activity of the anchored complex may be due to uniform distribution of metal centers on the polymer matrix, and/or an increased availability of styrene molecules which may adsorb on the polymer, close to the catalyst. The recyclability of the polymer anchored complexes **25** and **26** was checked up to two additional cycles after washing the catalysts with acetonitrile and drying after every use. No appreciable loss in the activities (see table 7), indicates that actual structures of the metal complexes remain unchanged, and that the catalysts remain equally active.

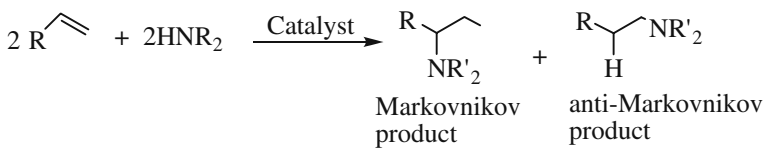

Scheme 16. Hydroamination of olefins producing the Markovnikov- or anti-Markovnikov-type product.

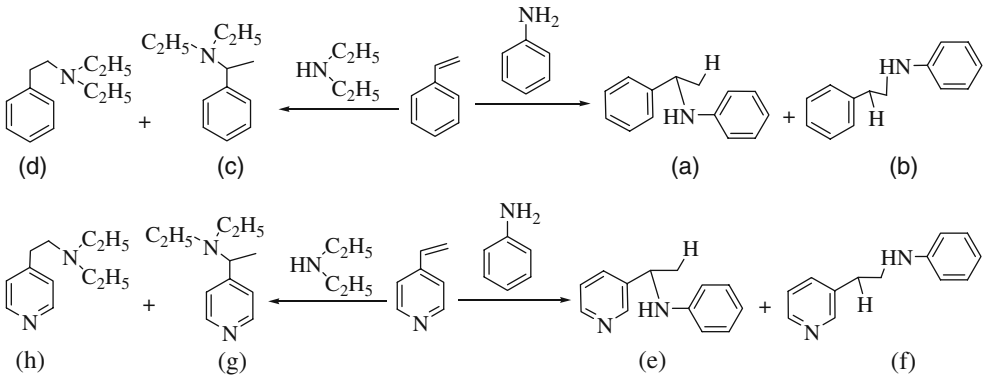

Scheme 17. (a) N-(1-phenylethyl)aniline, (b) N-phenethylaniline, (c) N,N-diethyl-1-phenylethanamine, (d) N,N-diethyl-2-phenylethanamine, (e) N-(1-(pyridin-3-yl)ethyl)aniline, (f) N-(2-(pyridin-3-yl)ethyl)aniline, (g) N,N-diethyl-1-(pyridin-4-yl)ethanamine, (h) N,N-diethyl-2-(pyridin-4-yl)ethanamine.[29]

Table 7. Conversion (%) and type of reaction products obtained using neat and anchored catalysts.[29]

Catalyst	Olefin	Amine	% Conv.	TOF (h^{-1})	% Selectivity	
					Markov. product	Anti-Markov. product
25	Styrene	Aniline	66	47	22	78
25[a]			65	-	22	78
25[b]			64	-	21	79
25		Diethylamine	48	34	27	73
25[a]			47	-	26	74
25[b]			45	-	26	74
25	Vinylpyridine	Aniline	82	59	18	82
25[a]			82	-	17	83
25[b]			81	-	16	84
25		Diethylamine	60	43	12	88
25[a]			60	-	11	89
25[b]			59	-	10	90
26	Styrene	Aniline	76	65	14	86
26[a]			75	-	14	86
26[b]			74	-	13	87
26		Diethylamine	60	50	29	71
26[a]			58	-	28	72
26[b]			58	-	27	73
26	Vinylpyridine	Aniline	92	77	19	81
26[a]			92	-	18	82
26[b]			91	-	18	82
26		Diethylamine	71	59	23	77
26[a]			70	-	23	77
26[b]			69	-	22	78
17	Styrene	Aniline	53	21	33	67
17		Diethylamine	31	12	35	65
17	Vinylpyridine	Aniline	69	27	30	70
17		Diethylamine	46	36	24	76
18	Styrene	Aniline	66	22	26	74
18		Diethylamine	42	13	34	66
18	Vinylpyridine	Aniline	88	27	32	68
18		Diethylamine	64	20	25	75

[a]First cycle of used catalyst
[b]Second cycle of used catalyst

5. Conclusions

Structural models of vanadate-dependent haloperoxidases (VHPO), where vanadium(V) is covalently linked to the imidazole-N, benzimidazole-N, pyridine-N or hydrazide-N, are presented. These model complexes exhibit interesting oxidative bromination and sulfoxidases activities, thus behaving as functional models as well. Immobilisation of these model complexes on chloromethylated polystyrene cross-linked with 5% divinylbenzene enhances the catalytic turn over numbers of these complexes along with their recyclable properties. These neat as well as polymer-supported complexes are also good catalysts for other organic transformations.

Acknowledgements

Financial assistances from the Department of Science and Technology (DST), New Delhi 110016 and Council of Scientific and Industrial Research (CSIR), New Delhi 110012 are gratefully acknowledged.

References

1. Weyand M, Hecht H J, Kiess M, Liaud M F, Vilter H and Schomburg D 1999 *J. Mol. Biol.* **293** 595
2. Carter-Franklin J N, Parrish J D, Tchirret-Guth R A, Little R D and Butler A 2003 *J. Am. Chem. Soc.* **125** 3688
3. Rehder D, Santoni G, Licini G M, Schulzke C and Meier B 2003 *Coord. Chem. Rev.* **237** 53
4. Butler A 1999 *Coord. Chem. Rev.* **187** 17
5. Messershmidt A and Wever R 1996 *Proc. Natl. Acad. Sci. USA* **93** 392
6. Isupov M I, Dalby A R, Brindley A, Izumi Y, Tanabe T, Murshudov G N and Littlechild J A 2000 *J. Mol. Biol.* **299** 1035
7. Butler A, Clague M J and Meister G E 1994 *Chem. Rev.* **94** 625
8. Butler A 1999 *Bioinorganic catalysis* 2nd edn (eds) J Reedijk and E Boiwman (New York: Marcel Dekker) ch. 5
9. Rehder D 1999 *Coord. Chem. Rev.* **182** 297
10. Maurya M R 2003 *Coord. Chem. Rev.* **237** 163
11. Maurya M R, Kumar A, Manikandan P and Chand S 2004 *Appl. Catal. A Gen.* **277** 45
12. Maurya M R, Agarwal S, Bader C, Ebel M and Rehder D 2005 *Dalton Trans.* 537
13. Maurya M R, Sikarwar S and Manikandan P 2006 *Appl. Catal. A: Gen.* **315** 74
14. Maurya M R, Kumar U and Manikandan P 2007 *Eur. J. Inorg. Chem.* 2303
15. Ashikhmina E V, Rubtsova S A, Dvornikova I A and Kuchin A V 2009 *Russian J. Org. Chem.* **45** 1509
16. Volcho K P and Salakhutdinov N F 2009 *Russian Chem. Rev.* **78** 457
17. Maurya M R, Kumar A, Ebel M and Rehder D 2006 *Inorg. Chem.* 5924
18. Rehder D, Weidemann C, Duch A and Priebsch W 1988 *Inorg. Chem.* **27** 584
19. Maurya M R, Agarwal S, Bader C and Rehder D 2005 *Eur. J. Inorg. Chem.* 147
20. Maurya M R, Agarwal S, Abid M, Azam A, Bader C, Ebel M and Rehder D 2006 *Dalton Trans.* 937
21. Plass W, Pohlmann A and Yozgatli H K 2000 *J. Inorg. Biochem.* **80** 181
22. Hirao T 1997 *Chem. Rev.* **97** 2707
23. Messerschmidt A, Prade L and Wever R 1997 *Biol. Chem.* **378** 309
24. Westland A D, Haque F and Bouchard J-M 1980 *Inorg. Chem.* **19** 2255
25. Casný M and Rehder D 2004 *Dalton Trans.* 839
26. Macedo-Ribeiro S, Hemrika W, Renirie R, Wever R and Messerschmidt A 1999 *J. Biol. Inorg. Chem.* **4** 209
27. Cornman C R, Kampf J, Lah M S and Pecoraro V L 1992 *Inorg. Chem.* **31** 2035
28. Maurya M R, Arya A, Kumar A and Costa Pessoa J 2009 *Dalton Trans.* 2185
29. Maurya M R, Arya A, Kumar U, Kumar A, Avecilla F and Costa Pessoa J 2009 *Dalton Trans.* 9555
30. Maurya M R, Arya A, Kumar A, Kuznetsov M L, Avecilla F and Costa Pessoa J 2010 *Inorg. Chem.* **49** 6586
31. Meunier B 1992 *Chem. Rev.* **92** 1411
32. Sherrington D C 1998 *Supported reagents and catalyst in chemistry* (eds) Hodnett B K, Keybett A P, Clark J H and Smith K (Cambridge: Royal Society of Chemistry) p. 220
33. Canali L and Sherrington D C 1999 *Chem. Soc. Rev.* **28** 85
34. de Miguel Y R 2000 *J. Chem. Soc. Perkin Tans. I* 4213
35. Leadbeater N E and Marco M 2002 *Chem. Rev.* **102** 3217
36. Punniyamurthy T and Rout L 2008 *Coord. Chem. Rev.* **252** 134
37. Gupta K C, Sutar A K and Lin C-C 2009 *Coord. Chem. Rev.* 1926
38. Maurya M R, Kumar M and Sikarwar S 2008 *Catal. Commun.* **10** 187
39. Rehder D, Santoni G, Licini G M, Schulzke C and Meier B 2003 *Coord. Chem. Rev.* **237** 53
40. Zampella G, Fantucci P, Pecorao V L and De Gioia L 2005 *J. Am. Chem. Soc.* **127** 953
41. Smith T S II and Pecoraro V L 2002 *Inorg. Chem.* **41** 6754
42. Hulea V and Dumitriu E 2004 *Appl. Catal. A: Gen.* **277** 99
43. Johnson J S and Bergman R G 2001 *J. Am. Chem. Soc.* **123** 2923
44. Li Y and Marks T J 1996 *J. Am. Chem. Soc.* **118** 9295
45. Beller M, Trauthwein H, Eichberger M, Breindl C and Müller T E 1999 *Eur. J. Inorg. Chem.* 1121
46. Nobis M and Driessen-Holscher B 2001 *Angew. Chem., Int. Ed.* **40** 3983